

# Water dynamics in charged and uncharged polysaccharide gels by quasi-elastic neutron scattering

H.D. Middendorf<sup>a</sup>, D. Di Cola<sup>b</sup>, F. Cavatorta<sup>b</sup>, A. Deriu<sup>b</sup>, C.J. Carlile<sup>c</sup>

<sup>a</sup> Clarendon Laboratory, University of Oxford, Oxford OX1 3PU, UK

<sup>b</sup> Dipartimento di Fisica, Università di Parma, I-41300 Parma, Italy

<sup>c</sup> ISIS Pulsed Neutron Facility, Rutherford Appleton Laboratory, Chilton, Didcot OX11 0QX, UK

Received 15 November 1994; revised 20 January 1994; accepted 1 March 1994

---

## Abstract

Using a  $\mu\text{eV}$  neutron spectrometer we have studied the mobility of water in gels formed by two polysaccharides: agarose and hyaluronic acid. Agarose is a nearly uncharged polysaccharide; its gels are fairly stiff, quasi-random networks of fibre bundles. Hyaluronic acid is a highly charged polysaccharide capable of retaining large amounts of water in entangled meshworks with unusual rheological properties. We have analysed sets of quasi-elastic lineshapes broadened by two proton populations with different degrees of freedom. The resulting microscopic mobility parameters and their temperature dependence reveal a complex behaviour. The overall effect of the biopolymer network is to increase translational as well as rotational relaxation times, but the changes observed are not dramatic and cannot fully account for the strikingly different macroscopic properties of these gels. Local electrostatic interactions (over 3 to 20 Å) do not appear to influence significantly the rheological behaviour.

## 1. Introduction

The polysaccharides [1], by virtue of their remarkable polymorphism and hydrogen-bonding properties, form a variety of aqueous gels that are of considerable fundamental and practical interest. Highly hydrated biopolymer networks are, first of all, excellent model systems for investigating cooperative phenomena in hierarchically structured two-component systems [2]. Secondly, the viscoelastic and transport properties of pure polysaccharide gels resemble those of the more complex protein-cum-polysaccharide aggregates found in living tissues [3]. Thirdly, polysaccharide gels are used extensively as electrophoretic media in biochemistry and molecular biology [4]. Finally, such gels have a number of important applications in medicine and biotechnology [5].

In this paper we report first results from a comparative neutron scattering study of the water mobility in gels of agarose and hyaluronic acid, two polysaccharides of similar primary and secondary structure but very different Coulomb interactions along their hydrated chains. The molecular diffusivity and microviscosity of water around biological polyelectrolytes have been characterised only recently by spectrometers capable of providing highly resolved spatiotemporal data over the relevant parameter domain. In early neutron work on solutions of tobacco mosaic virus particles [6] and on agarose gels [7] it was shown that the rotational correlation times in gel water are longer than those in pure water, but the low resolution of the instruments used did not permit detailed lineshape analyses of the quasi-elastic scattering. The results presented here are from a state-of-the-art backscattering spectrometer on a high-intensity pulsed neutron source.

## 2. Agarose and hyaluronate

The building blocks of these important polysaccharides are saccharide heterodimers; in the case of agarose they consist of  $\beta$ -1,4 linked D-galactose and  $\alpha$ -1,3 linked 3,6-anhydro-L-galactose, whereas hyaluronic acid dimers consist of  $\beta$ -1,3 linked D-glucuronic acid and  $\beta$ -1,4 linked N-acetyl-D-glucosamine. Pure, nearly sulfur-free agarose aggregates into a quasi-random network made up of relatively stiff bundles of uncharged double-helical chains [8,9]. These helices possess left-handed threefold symmetry with a 19 Å pitch. The network nodes are somewhat tangled ‘junction zones’ where double helices or separated strands pass through and interconnect without covalent branching. The result is a ‘physical’ gel, i.e. a large-scale thermoreversible structure held together solely by hydrogen-bonding, not chemical cross-linking. The relative strength of this 3D network, its pore size distribution, and the solid-like macroscopic properties combine to make agarose gels ideal for electrophoretic applications, in particular for the separation of large DNA fragments [4]. We have previously used small-angle neutron diffraction to characterise fractal aspects of the polysaccharide network in agarose gels [10,11].

Hyaluronic acid (HA) possesses an equally high density of potential hydrogen-bonding sites (OH-groups and certain oxygens), but in addition it is a strongly polyanionic molecule due to  $K^+$  or  $Na^+$  ions complexed between three or four helical polysaccharide strands. Electrostrictive forces in the primary hydration shell, in particular on water molecules close to these salt ions, may be expected to dominate the microscopic hydration properties of HA [12]. HA forms strikingly viscoelastic solutions at concentrations as low as 0.1% (a viscoelastic ‘putty’ [13]). This supports the rôle proposed for HA as a major component of the extended water-retaining network of polysaccharides and proteoglycans that make up the gel-like extracellular matrix of mammalian connective tissues [3]. The molecular conformation of HA is reasonably well known from numerous studies. Slightly hydrated fibre samples may show a double-helical structure, but a variety of chain conformations and packing arrangements have been obtained: two, three, and fourfold helical structures can be stabilised by suitable choice of temperature, humidity and ionic milieu, although in

moderately dilute solutions a substantial fraction of HA may remain in random coil conformation.

## 3. Experimental

The pulsed-source spectrometer IRIS [14] at the Rutherford Appleton Laboratory was used to measure quasi-elastic neutron spectra from gel samples and from pure water as a reference. IRIS is an inverted-geometry backscattering spectrometer on the 800 MeV spallation source ISIS; it employs a 36 m flight path and two crystal analyser arrays in near-backscattering geometry ( $\approx 175^\circ$ ). These analyser arrays produce 102 2000-point spectra with energy resolutions  $\delta E = 11 \mu\text{eV}$  (Mica006) and  $15 \mu\text{eV}$  (PG002) FWHM, respectively. The momentum transfer  $\hbar Q = \hbar(4\pi/\lambda)\sin\theta$  ranges from 0.3 to  $1.85 \text{ \AA}^{-1}$ ; its resolution  $\delta Q$  varies from  $0.02 \text{ \AA}^{-1}$  (lowest  $Q$ ) to  $0.04 \text{ \AA}^{-1}$  (high  $Q$ ). For comparable acquisition times (6 to 8 h), the quality of IRIS spectra is significantly better than that of spectra from first-generation backscattering instruments. The ratio of energy window to resolution width is an important parameter in work of this kind, since the  $Q$ -dependent sets of spectra acquisitioned simultaneously reflect a whole range of processes from translational diffusion (central-peak broadenings at low  $Q$ ) to rotational motions (large high- $Q$  broadenings, filling the entire window). This ratio is around 100 for both analyser arrays.

Because of the large  $n$ -p incoherent cross section (79.7 barn), the contribution of coherent scattering is negligible for all highly  $H_2O$ -hydrated biopolymer samples. Therefore the spectra obtained are essentially proportional to proton incoherent dynamic structure factors, or scattering laws,  $S_{\text{inc,p}}(Q, \omega)$  [15,16]. They represent double Fourier transforms of the ‘self’ part of the van Hove space-time correlation function for proton motions,  $G_{\text{s,p}}(r, t)$ . The space-time domain covered by the data discussed in this paper extends from  $\approx 3$  to  $20 \text{ \AA}$  and  $\approx 5$  to  $1000 \text{ ps}$ .

Our experiments required gel samples in the form of  $0.3 \times 40 \times 40 \text{ mm}^3$  slabs. Agarose gels were prepared by cooling a dilute solution (1%) of agarose from  $95^\circ\text{C}$  to room temperature. A method of applying moderate pressure to 1% slabs and absorbing water successively was used to obtain samples with concentrations up to 20%. Hyaluronate gels were prepared by slowly dilut-

ing Na-hyaluronate with distilled water in an aluminum sample holder, at room temperature. The unbuffered gels obtained in this way were acidic: the measured pH was 4.2 for a 1% HA gel. Dilute aqueous HA solutions ( $C \leq 10^{-3}$ ) have a pH of about 4.5. Raw IRIS spectra were normalised and corrected according to standard procedures, including a first-order multiple-scattering correction [15].

#### 4. Data analysis and interpretation

The simplest approach to the analysis of QENS spectra from highly hydrated biopolymers is to assume a composite scattering law according to a division of the total proton population into two or more groups with different mobility characteristics [17]. In previous work on QENS from heterogeneous macromolecular systems [16,18], the poor  $Q$ -resolution and narrow  $\hbar\omega$  window of conventional backscattering spectrometers made it difficult or impossible to go beyond simple two-component models for  $S_{\text{inc,p}}(Q, \omega)$ . The quality and dynamic range of data from IRIS is such that interpretations based on more complex model functions are now within reach.

Inspection of our QENS spectra from polysaccharide gels revealed the presence of at least three lineshape components: a narrow, nearly elastic component of low intensity, sitting on top of a broader line whose width depends markedly on  $Q$ , and a third component in the form of a very broad underlying feature which at all  $Q$  values fills the entire  $\hbar\omega$  window accessible through the PG002 analyser option. As an example we show in Fig. 1 a set of quasi-elastic lineshapes measured for a HA gel with  $C = 8\%$  at  $T = 278.5$  K, and further in Fig. 2 a single spectrum together with the components resulting from lineshape analysis based on the  $S_{\text{inc,p}}(Q, \omega)$  model described in detail below. Guided by the interpretation developed in earlier QENS studies of pure  $\text{H}_2\text{O}$  [19], we attribute the component with a  $Q$ -dependent broadening to translational diffusive motions, while the broader, nearly  $Q$ -independent part of the spectrum is regarded as due to rotational motions. Considering the large difference in broadening between these two components, there is some justification in adopting the conventional assumption of decoupled translational, rotational and vibrational degrees of freedom.

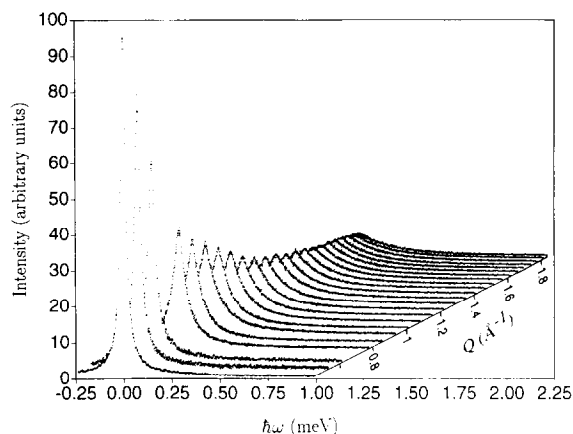


Fig. 1. Set of quasi-elastic spectra from an IRIS run for a 8% HA gel at  $T = 278$  K ( $Q$ -range  $1.1$ – $1.75$   $\text{\AA}^{-1}$ ). For clarity, only the  $\hbar\omega$  interval from  $-245$  to  $+245$   $\mu\text{eV}$  is shown.

To formulate a more detailed model for  $S_{\text{inc,p}}(Q, \omega)$ , we consider a partitioning of the sample volume into three distinct regions whose proton populations possess qualitatively different mobility characteristics. In region I, protons do not move appreciably over the longest time scale probed by IRIS ( $\approx 2 \times 10^{-9}$  s): these protons belong to the polymer backbone and to the fraction of very closely associated, essentially irrotationally ‘bound’ water molecules. A second region contains protons site-bound for times of the order of  $10^{-9}$  s and capable of performing only hindered rotations in a restricted space. Finally, in the interstitial aqueous phase proper (region III), we have a popula-

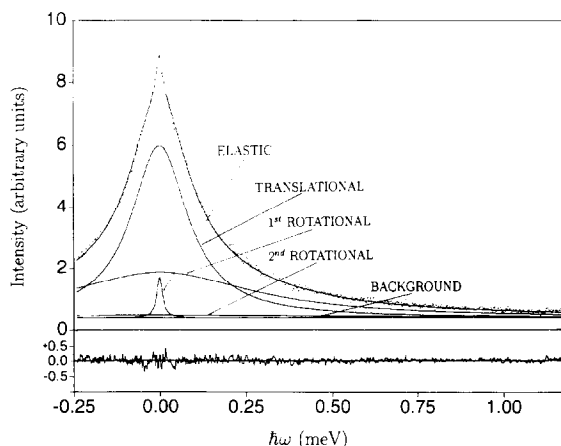


Fig. 2. Example of the decomposition of a lineshape ( $Q = 1.5$   $\text{\AA}^{-1}$ ) into elastic, translational and two rotational components for an 8% HA gel at  $T = 278$  K. The residuals obtained from the fitting are also shown.

tion of protons with translational and rotational degrees of freedom similar to bulk water protons but characteristic times that will depend on their proximity to a biopolymer fibre and the presence or absence of medium-range (up to 5 or 10 Å) electrostatic interactions. Based on this qualitative picture we may write a composite scattering law as follows:

$$S(Q, \omega) = f^I W^I \delta(\omega) + f^{II} W^{II} S_{\text{rot}}(Q, \omega) + f^{III} W^{III} [S_{\text{trans}}(Q, \omega) \otimes S_{\text{rot}}(Q, \omega)]. \quad (1)$$

In this expression the population factors  $f$  satisfy  $f^I + f^{II} + f^{III} = 1$ ,  $S_{\text{rot}}$  and  $S_{\text{trans}}$  are area-normalised incoherent scattering laws, and the  $W^i = \exp(-Q^2 \langle u_p^2 \rangle_i / 3)$  are Debye–Waller (DW) factors,  $\langle u_p^2 \rangle_i$  being an averaged mean-square proton vibrational displacement [15,18]. For  $S_{\text{trans}}$  the classical Chudley–Elliott (CE) model [20] of jumps to a random, radially symmetric distribution of sites  $\xi(r) \sim \exp(-r/r_0)$  gives

$$S_{\text{trans}}(Q, \omega) = (1/\pi) \Gamma_t(Q) / [\omega^2 + \Gamma_t^2(Q)],$$

$$\Gamma_t(Q) = D_t Q^2 / (1 + D_t Q^2 \tau_0), \quad (2)$$

where  $D_t$  is a translational diffusivity,  $\tau_0$  a residence time, and  $D_t = \langle r^2 \rangle / 6\tau_0$ . The rotational contribution

$S_{\text{rot}}(Q, \omega)$  may be described by the Sears model [21] for scattering from continuous rotational diffusion:

$$S_{\text{rot}}(Q, \omega) = j_0^2(Qa) \delta(\omega) + \sum_{\ell} (2\ell + 1) j_{\ell}^2(Qa) \ell(\ell + 1) \Gamma_r / [\omega^2 + (\ell(\ell + 1) \Gamma_r)^2]. \quad (3)$$

Here  $j_{\ell}$  is a spherical Bessel function of order  $\ell$ , and  $a$  an average radius of rotation identified with the water proton to centre-of-gravity distance, 0.94 Å. Three terms of the Sears expansion proved to be sufficient for the  $Q$  range and energy window covered by the PG002 analyser array.

In order to isolate the significant physical parameters with view on setting up efficient fitting procedures, we make the following assumptions. Since  $W^{II}$  and  $W^{III}$  affect the two mobile proton fractions in the same way, we set them equal. For the low gel concentrations of our experiment we expect  $(f^I + f^{II})$  to be  $\ll f^{III}$ , and this is borne out by the model fitting (compare Tables 1 and 2). As a consequence we only need a rough estimate of  $W^I$  (which is likely to be somewhat smaller than  $W^{II}$  and  $W^{III}$ ). Furthermore, the broad rotational contribution from fraction II protons, for the dilute gels

Table 1

Jump diffusion parameters (residence times  $\tau_0$ , diffusion coefficients  $D_t$ ) for the third proton population in agarose gels at different concentrations and temperatures. The calculated standard deviations give relative errors of about 10% for  $\tau_0$  and 5% for  $D_t$ . Activation energies are determined for  $T > 270$  K, and proton population factors are also reported

$T$ (K)	$D_t \times 10^5$ (cm <sup>2</sup> /s)			$\tau_0$ (ps)		
	$C = 1\%$	$C = 5\%$	$C = 10\%$	$C = 1\%$	$C = 5\%$	$C = 10\%$
269	1.06		0.91	59.2		23.0
270	1.37		1.29	14.5		8.9
	1.60	1.52	1.37	2.9	3.2	3.7
280	1.82	1.75	1.52	2.5	2.6	3.2
285	2.05			2.3		
294	2.20	2.11	2.05	2.0	2.4	2.8
305	2.74	2.58	2.43	1.8	2.0	2.6
325	3.50	3.43	3.34	1.5	1.8	2.0
$E_{\text{act}}$ (kcal/mol)	2.7	2.8	3.1	2.2	1.9	1.9
$f^I + f^{II}$	0.0006	0.012	0.045			
$f^{III}$	0.994	0.988	0.955			

Table 2

Same as Table 1, but for hyaluronate gels

<i>T</i> (K)	<i>D<sub>i</sub></i> × 10 <sup>5</sup> (cm <sup>2</sup> /s)			<i>τ</i> <sub>0</sub> (ps)		
	<i>C</i> = 0%	<i>C</i> = 1%	<i>C</i> = 8%	<i>C</i> = 0%	<i>C</i> = 1%	<i>C</i> = 8%
267	1.14	1.25		3.1	4.6	
271	1.09	1.38		2.4	3.6	
278	1.63	1.72	1.52	1.8	2.8	4.1
293	2.43	2.46	2.41	1.2	1.8	2.8
<i>E</i> <sub>act</sub> (kcal/mol)	4.6	4.1	5.1	3.3	5.3	4.1
<i>f</i> <sup>I</sup> + <i>f</i> <sup>II</sup>		0.002	0.008			
<i>f</i> <sup>III</sup>		0.998	0.992			

considered, is < 2% of the total rotational contribution and is negligible when considering the relative intensities of the terms contributing to the rotational structure factors  $A_\ell(Q) = (2\ell + 1)j_\ell^2(Qa)$  in the Sears expansion. With these assumptions we obtain:

$$S(Q, \omega)$$

$$= \exp(-\langle u_p^2 \rangle Q^2 / 3) \{ (f^I + f^{II}) \delta(\omega) + (1 - f^I - f^{II}) [S_{\text{trans}}(Q, \omega) \otimes S_{\text{rot}}(Q, \omega)] \}. \quad (4)$$

For comparison with measured sets of spectra, the  $Q = \text{const.}$  lineshapes resulting from this scattering law were first convoluted with resolution lines modelling the instrumental response function, as measured for a 2 mm vanadium scattering standard. An  $\omega$ -independent instrumental background was taken into account at this step. The fitting to sample spectra was performed in two stages: in the first step we determined starting values for the four physical parameters in Eq. (4) ( $\langle u_p^2 \rangle$ , one independent population factor, one translational and one rotational width) plus a flat background, without any constraint. This fit gave values for the rotational relaxation times  $\tau_r = 1/6\Gamma_r$  that turned out to be almost  $Q$ -independent, as expected; the temperature dependence of the  $Q$ -averaged values of  $\tau_r$  were then fitted to an Arrhenius law. In a subsequent fit the  $Q$ -averaged  $\tau_r$  values were kept constant and set equal to values derived from the Arrhenius-law fitting. This allowed a more precise determination of the  $Q$ -dependent translational broadening  $\Gamma_t(Q)$  and of the microscopic dif-

fusivity parameters  $D_i$  and  $\tau_0$ . The fitting routine used standard  $\chi^2$ -minimisation procedures with gradient techniques; details of the fitting programs will be published elsewhere [22].

## 5. Results and discussion

To begin with, the mean-square displacements  $\langle u_p^2 \rangle$  derived from the average proton Debye–Waller factor depend only slightly on gel concentration  $C$  and on temperature in the ranges examined. For both agarose and HA at room temperature we find  $\langle u_p^2 \rangle^{1/2} = 0.46 \pm 0.05$  Å. This value is in reasonable agreement with those measured for agarose gels using non-resonant Rayleigh–Thompson scattering of Mössbauer radiation (RSMR technique) [23]. It is also quite close to that measured by QENS for pure supercooled H<sub>2</sub>O [19,24].

In the following we will focus on the parameters which describe the diffusive dynamics of the mobile protons (group III). The random jump model for proton diffusion describes fairly well the overall  $Q$  dependence of the translational broadening  $\Gamma_t(Q)$  in the  $Q$  range covered. This is illustrated in Fig. 3 which shows the result of fitting curves based on Eq. (2) to  $\Gamma_t(Q)$  as obtained from a lineshape analysis of measured spectra for agarose and HA gels. An explanation for the weak oscillatory fine structure seen in the experimental data for agarose has been discussed elsewhere [17].

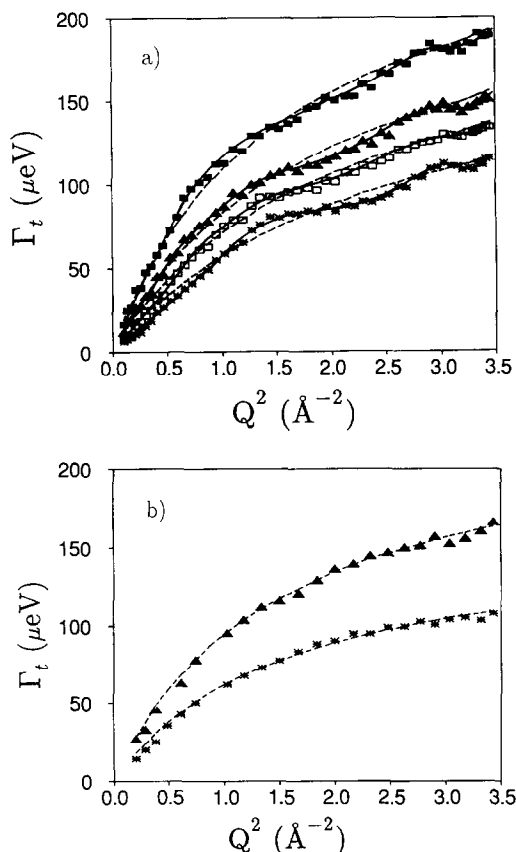


Fig. 3. Translational width  $\Gamma_t$  versus  $Q^2$  for (a) an agarose gel with  $C=1\%$  at different temperatures (top to bottom: 325, 306, 294, 286, 280, 276 K); (b) a HA gel with  $C=8\%$  at  $T=293$  K (upper) and 278 K (lower). Dashed curves are fits to a Chudley–Elliott random jump model. The continuous lines in (a) are drawn as visual guides.

Such oscillations are less conspicuous in hyaluronic acid, and more data on HA are needed to substantiate this point.

From the values of  $\Gamma_t(Q)$  we have derived the translational diffusivity parameters  $D_t$  and  $\tau_0$  based on the CE model; they are summarised in Table 1 (agarose) and Table 2 (hyaluronate) together with the activation energies and the population factors ( $f^I + f^{II}$ ) and  $f^{III}$ . In Fig. 4 we compare residence times  $\tau_0$  measured for agarose and hyaluronate gel water with those for pure supercooled water derived from recent QENS measurements using IRIS [24]. Gel water is always less mobile than pure  $\text{H}_2\text{O}$ , and this is manifest in longer residence times for jump diffusion. The molecular dynamics of gel water shows some qualitative differences with respect to pure  $\text{H}_2\text{O}$ : above 273 K the tem-

perature dependence of  $\tau_0$  suggests a lowered activation energy relative to  $\text{H}_2\text{O}$ . In agarose gels, at a temperature  $T^* \approx 273$  K, we observe a ‘knee’ where  $\tau_0$  rapidly increases with a markedly non-Arrhenius behaviour (Fig. 4). In this region gel water is much less mobile than supercooled  $\text{H}_2\text{O}$ ; the small but measurable translational broadenings indicate that it is not ice-like. The values of  $\tau_0$  in hyaluronic acid gels are very close to those in agarose gels (Fig. 4). The main differences are, first, that the curvature of  $\tau_0(Q)$  is smaller for HA and closer to that of pure water, and secondly, there seems to be no transition to a steeper  $T$  dependence down to the lowest temperature investigated,  $T=267.5$  K. However, further data on HA gels below 267 K are needed to elucidate the low temperature behaviour of water in this system.

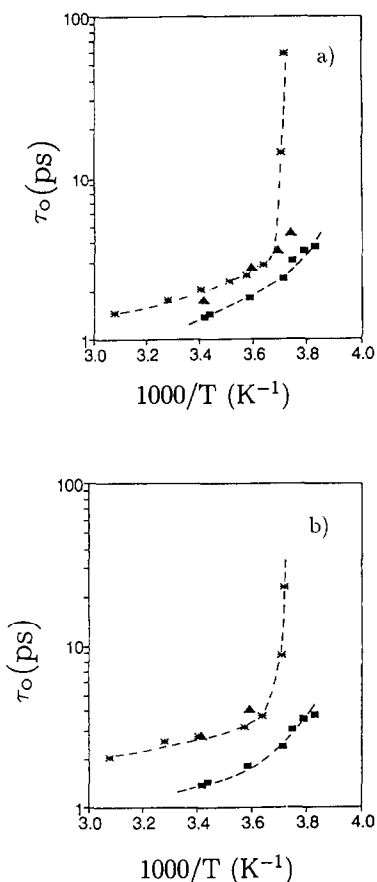


Fig. 4. Arrhenius plot of residence times  $\tau_0$  for pure  $\text{H}_2\text{O}$  (■), hyaluronic acid (▲) and agarose gel water (\*). Gel concentrations are 1% (a) and 8% (b).

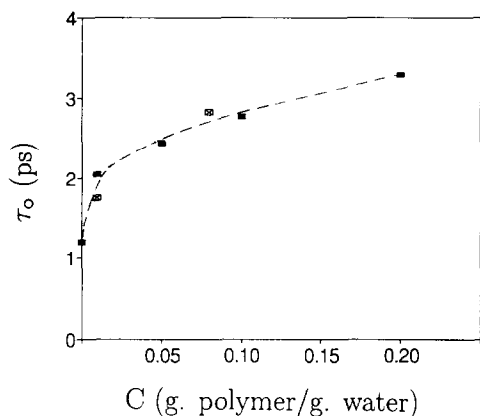


Fig. 5. Dependence on concentration  $C$  of residence times  $\tau_0$  for agarose (■) and HA (×) gel water at  $T = 293$  K.

Overall, for  $T > 270$  K, the temperature dependence of  $\tau_0$  in both gels resembles that of pure supercooled water at some corresponding temperature between 250 and 270 K. It is possible therefore to rescale the  $\tau_0(Q)$

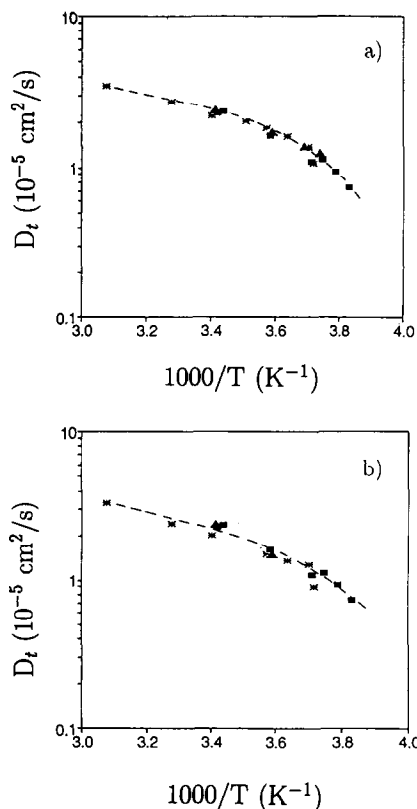


Fig. 6. Arrhenius plot of translational diffusion coefficients  $D_t$  for pure H<sub>2</sub>O (■), hyaluronic acid (▲) and agarose gels (\*). Gel concentrations are 1% (a) and 8% (b).

curves to a common 'universal' curve by assigning to gel water a 'structural temperature' lower than the actual thermodynamic temperature. Similar concepts have been put forward to describe the properties of hydration water in proteins and in other biomolecular environments [25,26]. It is also worth noting that for HA we obtain a  $\tau_0$  versus  $T/T^*$  curve much closer to that of pure water. The concentration dependence of  $\tau_0$  is very similar in HA and agarose gels (Fig. 5): the transition from the bulk water values to those in gels occurs in a fairly sharp manner between  $C = 0$  and 0.01. It appears that the polysaccharide network is capable of affecting the average translational mobility of water molecules even at very low concentrations.

The values of the microscopic water diffusivity  $D_t$  for the two gels are close to each other and to those for H<sub>2</sub>O. Above 273 K they vary linearly in an Arrhenius plot (Fig. 6), but with different activation energies for agarose and HA (Tables 1 and 2). Their dependence on biopolymer concentration  $C$  also differs sharply: for the HA gels we find that  $D_t(C)$  is essentially constant and equal to its pure water value of  $2.43 \times 10^{-5} \text{ cm}^2/\text{s}$ , whereas for agarose  $D_t$  first drops from its  $C = 0$  value (pure H<sub>2</sub>O) to the 1% gel value rather abruptly and then continues to decrease (Fig. 7).

The rotational relaxation time  $\tau_r$  is a parameter of the broad multi-Lorentzian that can be extracted from measured lineshapes by deconvolution according to Eq. (3). The amplitude of this component vanishes as  $Q \rightarrow 0$  and is small in  $Q$  regions where the rotational form factors  $A_\ell(Q)$  are  $\ll 1$ ; their contribution is quite small in the  $Q$  range analysed. Using the fitting proce-

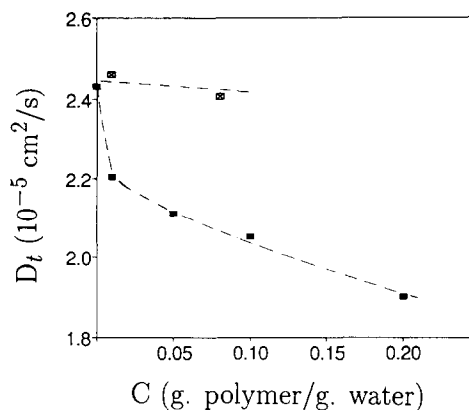


Fig. 7. Dependence on concentration  $C$  of translational diffusion coefficients  $D_t$  for agarose (■) and HA (×) gel water at  $T = 293$  K.

ture described above we have obtained values of  $\tau_r = 0.3\text{--}0.4$  ps at 293 K for agarose water whereas for hyaluronate  $\tau_r \approx 1$  ps, the estimated error being  $\approx 20\%$ . These values of  $\tau_r$  for both agarose and HA gel water depend only slightly on concentration. Their temperature variation is Arrhenius-like with an activation energy of 3.2 kcal/mol, a typical value for H-bond breaking. It is worth noting that  $\tau_r$  for HA is higher than for agarose and close to the value for pure  $\text{H}_2\text{O}$ . A more accurate determination of  $\tau_r$  could be obtained by collecting data over the widest energy window accessible by IRIS (graphite 004 reflection, up to  $\hbar\omega \approx 8$  meV).

## 6. Conclusions

A close look at the microscopic mobility of water in these two gels reveals a complex behaviour. Considering the structural and dynamical heterogeneity of aqueous polysaccharide gels in general, and of agarose versus hyaluronate in particular, this is not surprising. In agarose gels, the 3D network of polysaccharide fibre bundles is highly stable and the properties are solid-like even at very low concentrations. In HA, on the other hand, the absence of permanent crosslinks combined with a high density of charged groups gives fibrous networks with unique viscoelastic properties.

Our results indicate that the microscopic water dynamics differs in some important respects, but these differences are not dramatic. In order to understand this result one has to bear in mind that the molecular motions ‘seen’ in our experiments are in the psec to nsec region over distances from a few Å to  $\approx 20$  Å. The effect of the presence of the biopolymer network is to slow down the bulk water dynamics, and above 273 K the slopes of the  $\tau_0$  curves in Fig. 5 are lower for agarose gels than for pure  $\text{H}_2\text{O}$ . This may be correlated with the biopolymer matrices, which by their extended network of H-bonding sites act to increase the average size of the transient water clusters [17]. Such effects appear to be much weaker in HA gels: (i) the activation energies derived from the temperature dependence of both  $D_t$  and  $\tau_0$  are closer to pure water than those of agarose; (ii)  $D_t$  does not change appreciably on changing the HA concentration and has a value very close to that of  $\text{H}_2\text{O}$ ; (iii) the fraction of protons with highly reduced mobility is  $\approx 1/3$  of that found for agarose at comparable concentrations.

These differences may have some effect on the rheological properties, but cannot fully account for the strikingly different macroscopic properties of these two gels. Their macroscopic properties are unlikely to be due only to interactions over scale lengths of the order of 10 Å, and must involve larger structural elements by way of effects that relate more specifically to the disparate fibre aggregation and network connectivity properties, rather than differences in electrostatic field effects on the local proton dynamics. It should be noted, more generally, that differences in the microscopic dynamic behaviour of bulk and gel water must reflect qualitatively different cooperative interactions in the transient H-bond network of pure  $\text{H}_2\text{O}$  relative to  $\text{H}_2\text{O}$  ‘perturbed’ by a biopolymer component with a high density of OH groups.

## Acknowledgements

This work was supported by CNR (Italy), SERC (UK), The E.P.A. Cephalosporin Fund, and NATO.

## References

- [1] D. Parry and E.N. Baker, Rept. Progr. Phys. 47 (1984) 1133.
- [2] F. Brochard and P.G. de Gennes, J. Phys. Lettres 44 (1983) L-785.
- [3] S. Arnott and D.A. Rees, Glycosaminoglycan assemblies in the extracellular matrix (Humana, New York, 1982).
- [4] B.H. Zimm and S.D. Levene, Quart. Rev. Biophys. 25 (1992) 171.
- [5] D. De Rossi, K. Kajiwara, Y. Osada and A. Yamauchi, eds. Polymer gels, fundamentals and biomedical applications (Plenum Press, New York, 1991).
- [6] A.M. Hecht and J.W. White, J. Chem. Soc. Faraday Trans. II 72 (1976) 439.
- [7] E.C. Trantham, H.E. Rorschach, J.S. Clegg, C.F. Hazlewood, R.M. Nicklow and N. Wakabayashi, Biophys. J. 45 (1984) 927.
- [8] S. Waki, J.D. Harvey and A.R. Bellamy, Biopolymers 21 (1982) 1909.
- [9] G. Corongiu, S.L. Fornili and E. Clementi, J. Quant. Chem. 10 (1983) 277.
- [10] H.D. Middendorf, A. Deriu and F. Cavatorta, Progr. Colloid Polym. Sci. 81 (1990) 274.
- [11] A. Deriu, F. Cavatorta, D. DiCola and H.D. Middendorf, J. Phys. IV 3 (1993) C1-237.
- [12] S. Arnott, A.K. Mitra and S. Raghunathan, J. Mol. Biol. 169 (1983) 861.



- [13] I.C.M. Dea, R. Moorhouse, D.A. Rees, S. Arnott, J.M. Guss and E.A. Balasz, *Science* 179 (1973) 560; E.D.T. Atkins and J.K. Sheenan, *Science* 179 (1973) 562.
- [14] C.J. Carlile and M.A. Adams, *Physica B* 182 (1992) 431.
- [15] C.J. Windsor, *Pulsed neutron scattering* (Taylor and Francis, London, 1981).
- [16] H.D. Middendorf, *Ann. Rev. Biophys. Bioengineer.* 13 (1984) 425.
- [17] A. Deriu, F. Cavatorta, D. Cabrini, C.J. Carlile and H.D. Middendorf, *Europhys. Letters* 24 (1993) 351.
- [18] M. Bée, *Quasielastic neutron scattering* (Adam Hilger, Bristol, 1988).
- [19] J. Teixeira, M.-C. Bellissent-Funel, S.H. Chen and A.J. Dianoux, *Phys. Rev. A* 31 (1985) 913.
- [20] P.A. Egelstaff, *An introduction to the liquid state* (Academic Press, New York, 1967).
- [21] V.F. Sears, *Can. J. Phys.* 44 (1966) 1299; 45 (1967) 237.
- [22] F. Cavatorta and D. DiCola, in preparation.
- [23] G. Albanese, A. Deriu, F. Uguzzoli and C. Vignali, *Nuovo Cimento 9D* (1987) 319.
- [24] F. Cavatorta, A. Deriu, D. Di Cola and H.D. Middendorf, *J. Phys. Condens. Matter* 6 (1994) A113.
- [25] G. Nimtz, P. Marquardt, D. Stauffer and W. Weiss, *Science* 242 (1988) 1671.
- [26] R. Giordano, G. Salvato and U. Wanderlingh, *Phys. Rev. A* 41 (1990) 689.